Engineering Structures 150 (2017) 934–946

Contents lists available at ScienceDirect

Engineering Structures

journal homepage: www.elsevier.com/locate/engstruct

Development of box-shaped steel slit dampers for seismic retrofit of building structures

Joonho Lee, Jinkoo Kim *

Dept. of Civil and Architectural Engineering, Sungkyunkwan University, Suwon, Republic of Korea

ARTICLE INFO

Article history:
Received 4 December 2016
Revised 21 July 2017
Accepted 24 July 2017

Keywords:
Slit dampers
Seismic retrofit
Moment frames
Nonlinear analysis

ABSTRACT

In this study a steel slit damper is developed by combining four steel slit plates to be used for seismic retrofit of structures. The proposed damper consists of four slit plates integrated into a box shape, and can produce larger damping force in relatively small size compared with the conventional slit plate dampers composed of single slit plate. Cyclic loading tests of two damper specimens are carried out to evaluate their seismic energy dissipation capability. The slit dampers are applied to seismic retrofit of an existing reinforced concrete structure using the procedure developed based on the capacity spectrum method. Nonlinear dynamic analysis of the model structure shows that the dampers installed using the proposed procedure are effective in restraining the building displacement within a given target performance limit state. The time history of the hysteretic energy dissipation shows that most seismic energy is dissipated by the dampers while the structural elements mostly remain elastic.

1. Introduction

Metallic dampers are considered to be efficient and reliable energy dissipative devices for mitigating earthquake-induced damage in structures. They can be easily implemented in practice as no special fabrication technique or expansive material is involved. They have been developed in many forms such as ADAS [1], buckling restrained braces [2,3], honeycomb dampers [4], and steel plate dampers [5]. They are generally placed between stories where inter-story drifts are relatively large, and dissipate seismic energy by hysteretic behavior of vertical steel strips.

A steel plate slit damper has been applied for efficient seismic design and retrofit of building structures. Kobori et al. [6] developed hourglass and honeycomb type plate steel dampers to reduce the seismic response of buildings. Chan and Albermani [7] carried out cyclic loading test of steel slit dampers made from wide flange sections and verified their seismic energy dissipation capacity. Saffaria et al. [8] developed a slit damper for enhancing strength and ductility of post-Northridge connections. Seo et al. [9] investigated the effect of the slit damper made of a shape memory alloy. Kim and Jeong [10] presented a ductility-based seismic design procedure of steel plate slit dampers for seismic retrofit of asymmetric structures. Lee et al. [11,12] developed slit dampers with non-uniform strips to reduce stress concentration when subjected to cyclic loadings. Lee and Kim [13] and Kim and Shin [14] developed a steel slit damper combined with friction dampers and showed its efficiency by numerical analysis. According to the results of previous research, the steel slit dampers generally show reliable performance for earthquakes and their behavior can be precisely predicted using simple formulas derived from elementary structural mechanics.

In this study a steel slit damper is developed by combining four steel slit plates into a box shape to be used for seismic retrofit of structures. They are designed to be installed as knee or diagonal braces between stories. The proposed damper with four slit plates integrated into relatively small size can produce larger damping force compared with the conventional slit plate dampers composed of single slit plate. Cyclic loading tests of the dampers are carried out to evaluate their seismic energy dissipation capability. The slit dampers are designed for seismic retrofit of an existing reinforced concrete structure using the capacity spectrum method, and their applicability is verified by nonlinear dynamic analysis.

2. Performance of box-shaped slit dampers

2.1. Configuration and modeling of the dampers

A steel slit damper is developed by combining four steel plates with slits and internal and external steel casings into a box shape. One side of each steel plate with slits is bolted to the interior casing and the other side is connected to the exterior casing. A cap plate is

* Corresponding author.
E-mail address: jkim12@skku.edu (J. Kim).

http://dx.doi.org/10.1016/j.engstruct.2017.07.082
0141-0296/

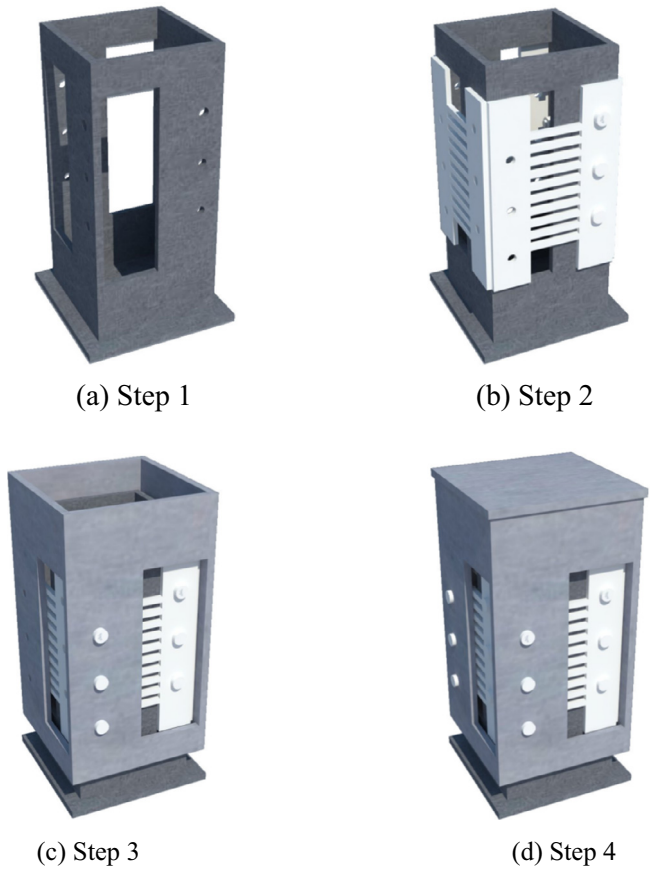

Fig. 1. Assembly sequence of the box-shaped slit damper.

welded to the exterior casing, and a bottom plate is welded to the interior casing. Fig. 1 shows the configuration and the assembly procedure of the box shaped slit damper. The damper is devised

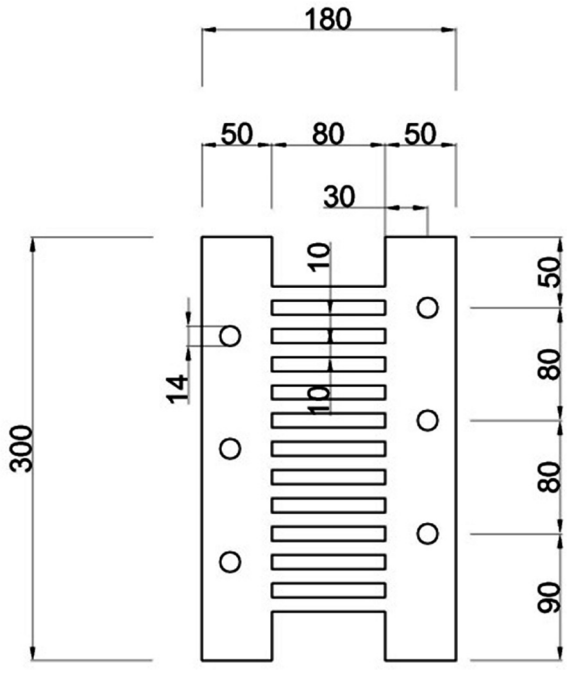

Fig. 2. Dimension of the steel plate with slits.

Table1
Dimensions of the box-shaped slit dampers.

Specimen	T (mm)	N	b (mm)	L_0 (mm)	b/L_0
1	8	10	10	80	0.125
2	16	10	10	80	0.125

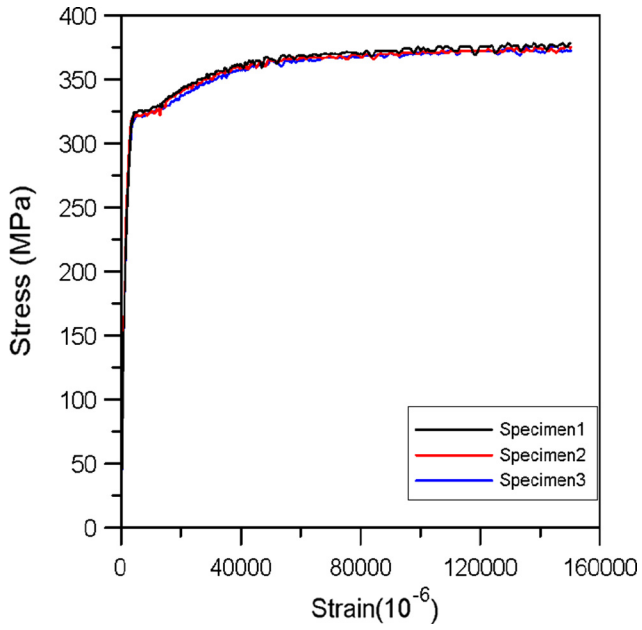

Fig. 3. Stress-strain curve of the steel obtained from coupon tests.

Table 2
Properties of the specimens.

Specimen	f_y (N/mm^2)	E (N/mm^2)	ε_y	P_y (N)	δ_y (mm)
1	325	205,000	0.00159	16,250	0.51
2	325	205,000	0.00159	32,500	0.51

Table 3
Axial displacements of the dampers installed with 30 and 45 degree slopes with beams corresponding to the three inter-story drift ratios.

Inter-story drift ratio	Displacement (mm)
(a) 30 degree	
5%	43.3
2.5%	21.7
2%	17.3
(b) 45 degree	
5%	35.4
2.5%	17.7
2%	14.1

to be installed as a knee brace at the beam-column joint. Fig. 2 shows the steel plate with slits having overall dimension of 180 × 300 mm with the length l_o and width b of slit column 80 mm and 10 mm, respectively. Two specimens are prepared with different plate thickness of 8 mm (specimen 1) and 16 mm (specimen 2). The number of slit column is 10 in both specimens. Table 1 shows the dimensions of the slit dampers. The overall dimension of the interior and the exterior casings of specimen 1 are 180 × 180 × 450 mm and 216 × 216 × 450 mm, respectively. The dimensions of the interior casing of specimen 2 are the same with those of specimen 1, and the dimensions of the exterior casing

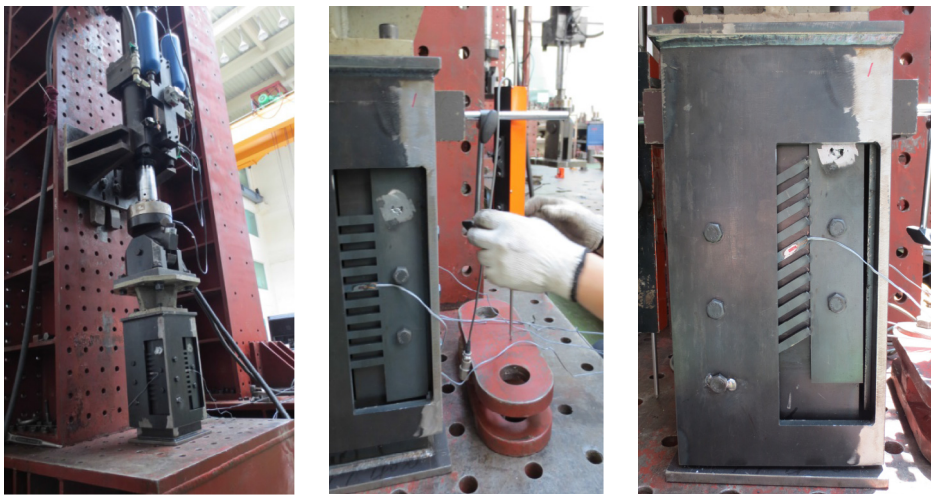

(a) Test setup (b) LVDT (c) At fracture

Fig. 4. Test setup of the box-shaped slit dampers.

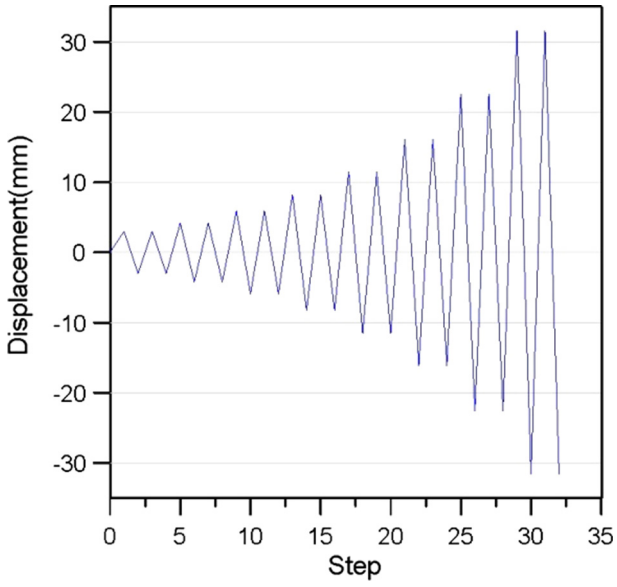

Fig. 5. Loading protocol used in the cyclic tests.

increase to 232 × 232 × 450 mm. The casings are made by welding 10 mm thick steel plates. Fig. 3 shows the stress-strain curves for steel obtained from tests of three coupons using a universal testing machine, where the mean yield and the ultimate strengths are 325.6 and 376.5 N/mm^2, respectively, and the elastic modulus is 205 kN/mm^2. These values are used in the nonlinear analysis of the slit dampers.

The stiffness and the yield strength of a slit damper can be derived as follows [7] based on the assumption that the slit columns are fixed at both ends:

$$k_s = n\frac{12EI}{l_o^3} = n\frac{Etb^3}{l_o^3} \tag{1a}$$

$$P_{ys} = \frac{2nM_p}{l_0} = \frac{nf_y tb^2}{2l_0} \tag{1b}$$

where n = number of strips, t = thickness of strips, b = width of strips, and l_o = length of the vertical strip. The yield strengths and the yield displacements of the specimens obtained from the coupon tests and the above equations are shown in Table 2. Table 3 shows the axial displacements of the specimens corresponding to various inter-story drift ratios when the dampers are installed with slopes of 30 and 45 degrees with the beam as knee braces.

2.2. Cyclic loading tests of the specimens

In this section the seismic performances of the two box-shaped slit dampers are investigated by cyclic loading test using a 300 kN hydraulic actuator. Fig. 4 depicts the test setup of the dampers. Two LVDTs (Linear variable differential transformers) are attached to the exterior casing to measure displacement. The loading protocol 1 for quasi-static cyclic testing provided in the FEMA-461M [14] and depicted in Fig. 5 is used in the tests. The minimum displacement Δ_0 is set to be 3 mm which corresponds to the inter-story drift ratio of 0.3% when the damper is located with the slope of 30 degree from the beam. The amplitude is increased by 1.4 times the previous one in each loading cycle. The maximum displacement is set to be 31.6 mm which is significantly larger than typical displacement in a knee brace subjected to a design level earthquake. Fig. 6 shows the hysteresis curves of the two specimens obtained from the loading tests, and Fig. 7 depicts the bi-linearization of the envelop curves of the hysteresis curves, which are used in the nonlinear analysis in the following sections. It is observed that the yield strength and displacement of specimen 1 are 63.2 kN and 1.8 mm, respectively, and the maximum strength is 100 kN. The maximum displacement before fracture is 31.6 mm. In specimen 2 the yield strength and yield displacement are 118 kN and 1.9 mm, respectively, and the maximum strength and displacement are observed to be 210 kN and 31.6 mm. The post-yield stiffness of specimens 1 and 2 are 1.8 and 3.0 kN/mm, respectively. The 110 % increase in the maximum strength of specimen 2 seems to be reasonable considering that the thickness of the slit plate in specimen 2 is twice the thickness of the slit plate in specimen 1. The maximum displacements of the two specimens at fracture are substantially larger than those expected under maximum considered earthquakes. The test results show that the dampers act stably during the cyclic loading test dissipating significant amount of seismic energy. No local buckling or out-of-plain buckling was observed in the slit plates and the internal and external casings. As the slit columns are subjected to bending deformation during the axial deformation of the damper, generally they are not

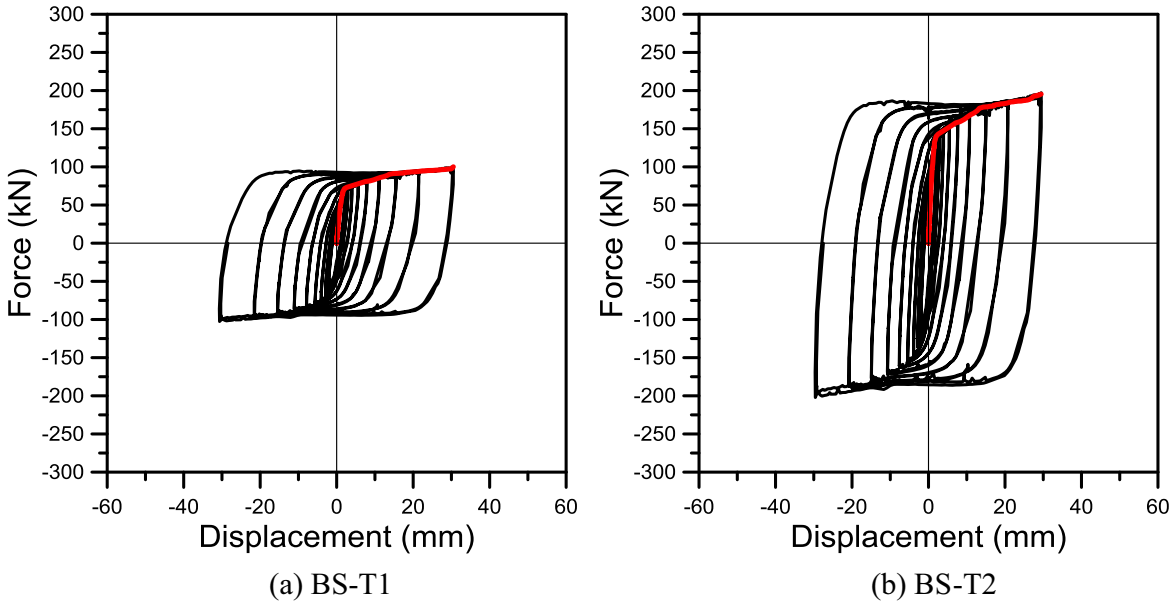

Fig. 6. Force-displacement curves of box-shaped slit dampers.

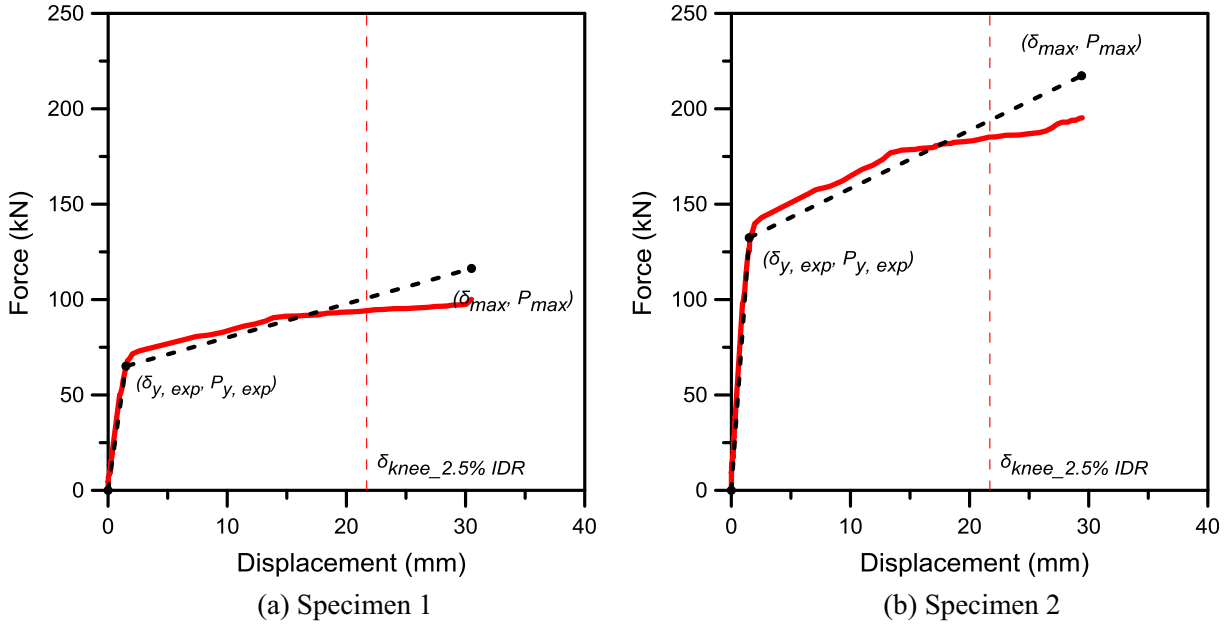

Fig. 7. Bi-linearization of the envelop curves of the test specimens.

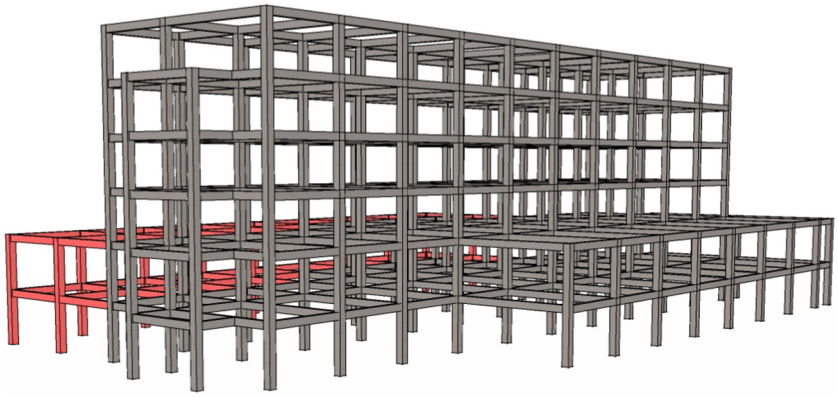

Fig. 8. 3D-view of the analysis model structure.

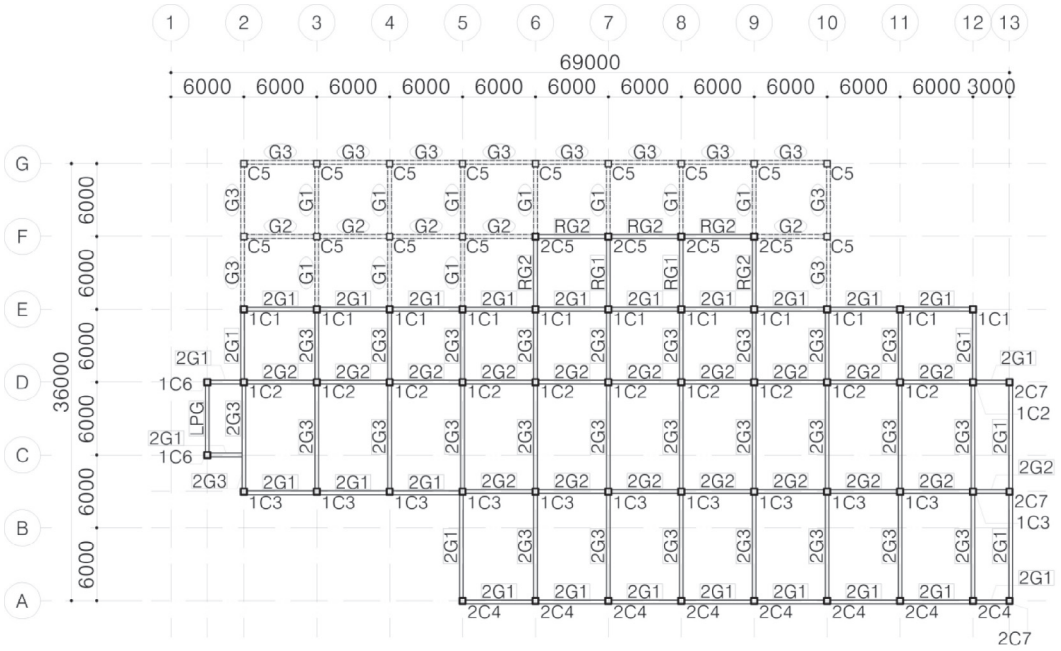

(a) 1st and 2nd stories

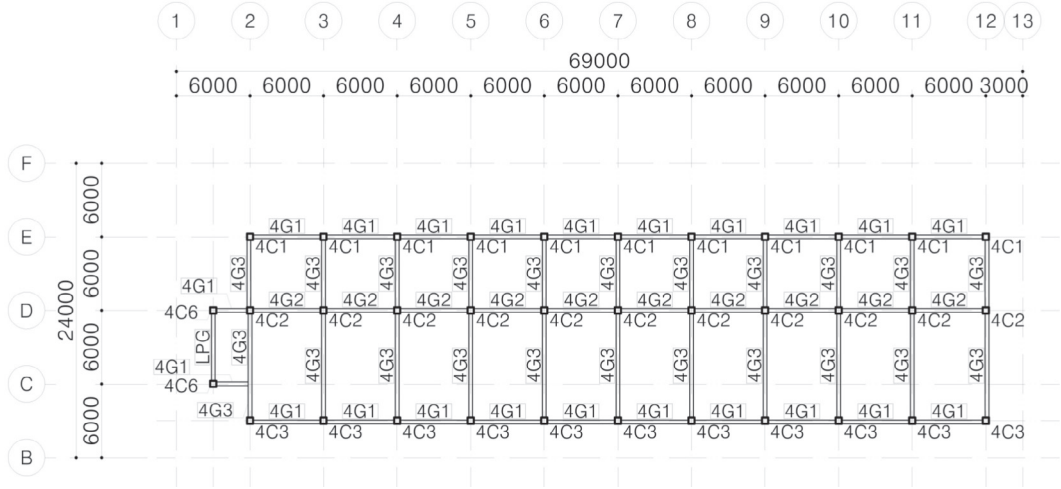

(b) 3rd~6th stories

Fig. 9. Structural plan of the analysis model structure.

Table 4
Sectional properties of 2nd and 6th story beams.

Section	Size (mm)	Rebar			
		Exterior (I, J)		Interior (M)	
		Bottom	Top	Bottom	Top
2G1	300 × 540	2-D19	6-D19	5-D19	2-D19
2G2	300 × 560	2-D19	8-D19	6-D19	2-D19
2G3	300 × 520	2-D19	7-D19	3-D19	2-D19
6G1	300 × 450	2-D19	5-D19	5-D19	2-D19
6G2	300 × 450	2-D19	8-D19	7-D19	2-D19
6G3	300 × 430	3-D19	8-D19	5-D19	3-D19

subjected to axial force. However, at large axial deformation of the dampers, slit columns may be subjected to some tensile force as well as bending moment depending on the damper configuration, as observed in the previous study on steel slit dampers [14] where the formation of the tension field contributed to increase of post-yield stiffness at large displacement. In this test, however,

Table 5
Sectional properties of columns.

Section	Size (mm)	Rebar	Section	Size (mm)	Rebar
1C1	450 × 450	8-D19	5C3 ~ 6C3	450 × 450	16-D25
2C1 ~ 4C1	400 × 400	8-D16	1C4 ~ 2C4	450 × 450	12-D22
5C1 ~ 6C1	350 × 350	8-D16	1C5 ~ 2C5	350 × 350	4-D22
1C2	650 × 650	16-D19	1C6	350 × 350	4-D22
2C2 ~ 4C2	600 × 600	12-D22	2C6 ~ 4C6	350 × 350	4-D22
5C2 ~ 6C2	550 × 550	16-D22	5C6	350 × 350	4-D22
1C3	500 × 500	12-D19	1C7 ~ 2C7	350 × 350	4-D22
2C3 ~ 4C3	450 × 450	8-D19	C5	350 × 350	8-D19

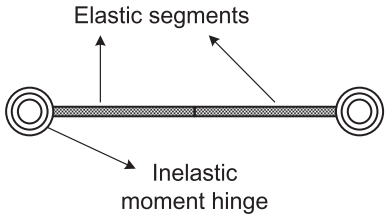

(a) Nonlinear model of beam elements

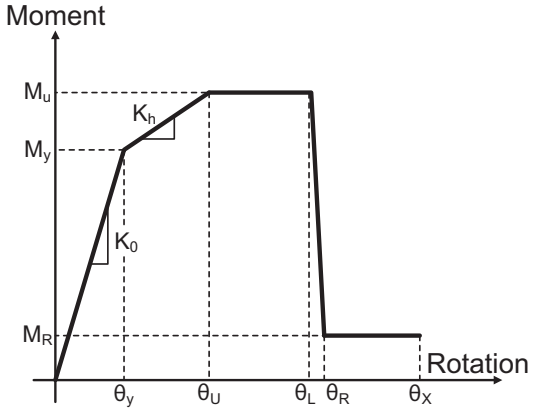

(b) Moment-rotation relationship

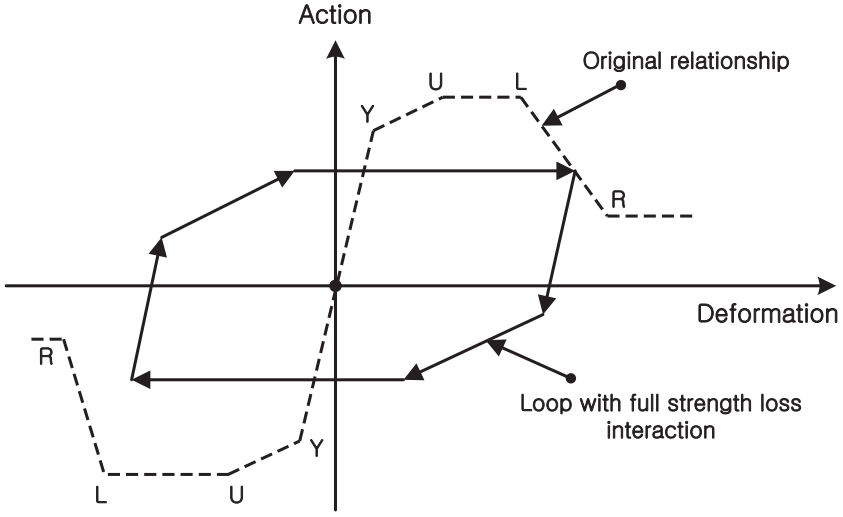

(c) Hysteresis loop

Fig. 10. Nonlinear model for RC beam elements.

no significant increase in post-yield stiffness was observed since the slit columns fractured in bending before occurrence of large displacement enough to induce tensile force in the slit columns.

3. Seismic retrofit of a RC moment frame with box-shaped slit dampers

3.1. Structural modeling and analysis of the model structure

The box-type slit dampers are applied to the seismic retrofit of a six-story reinforced concrete moment frame shown in Figs. 8 and 9 designed as a hospital building without considering seismic load. The building is designed using dead load of 3.68 kN/m^2 and live load of 3.0 kN/m^2. The ultimate strengths of concrete and rebars are 21 MPa and 400 MPa, respectively. The size and rebar information of selected beams and columns are presented in Tables 4 and 5, respectively.

The analysis model for RC beam elements is composed of two end rotation type moment hinges as shown in Fig. 10(a). The nonlinear behavior of the moment hinge is defined based on ASCE/SEI 41-13 [15] and is presented in Fig. 10(b). Fig. 10(c) shows the hysteresis curve of beam members with strength degradation. Fig. 11 shows the nonlinear models for RC columns subjected to monotonic and cyclic loads. The flexural and shear stiffness of the beams are reduced to 50% and 40% of the original values, respectively, as recommended in ASCE/SEI 41-13. The flexural stiffness of the columns is reduced to 50% or 70% of the original value depending

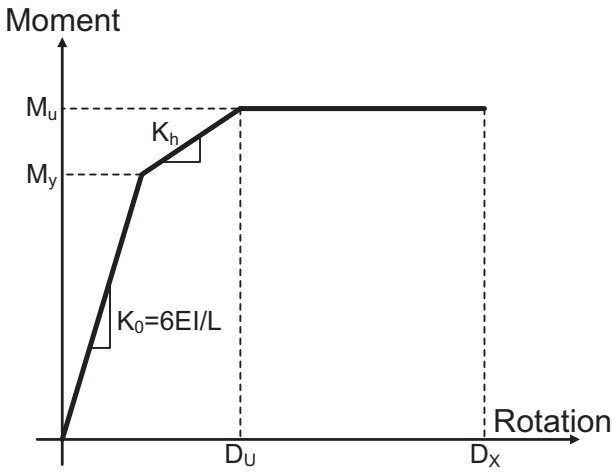

(a) Moment-rotation relationship

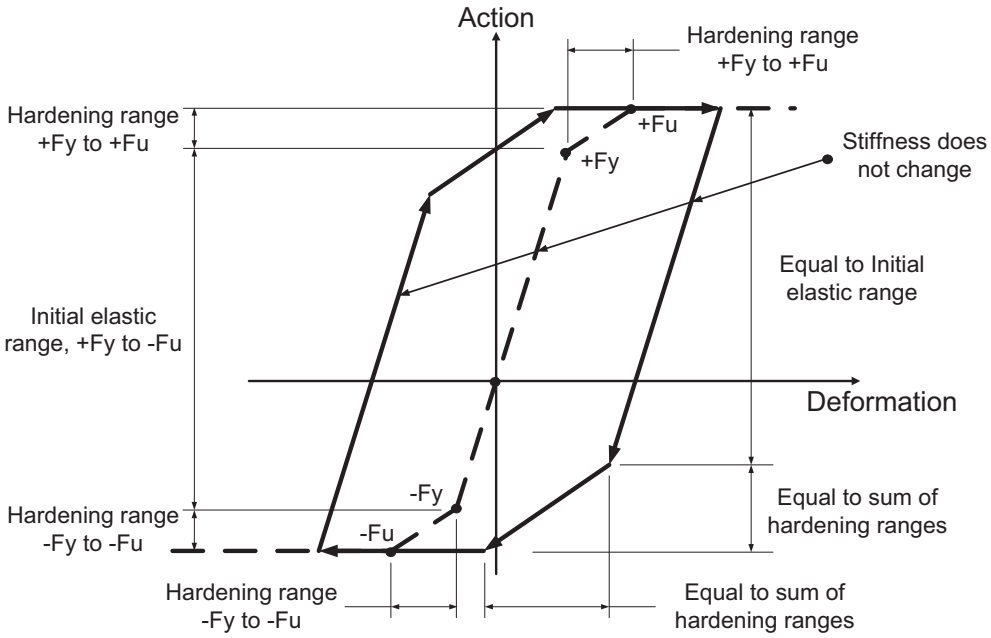

(b) Hysteresis loop

Fig. 11. Nonlinear model for RC columns.

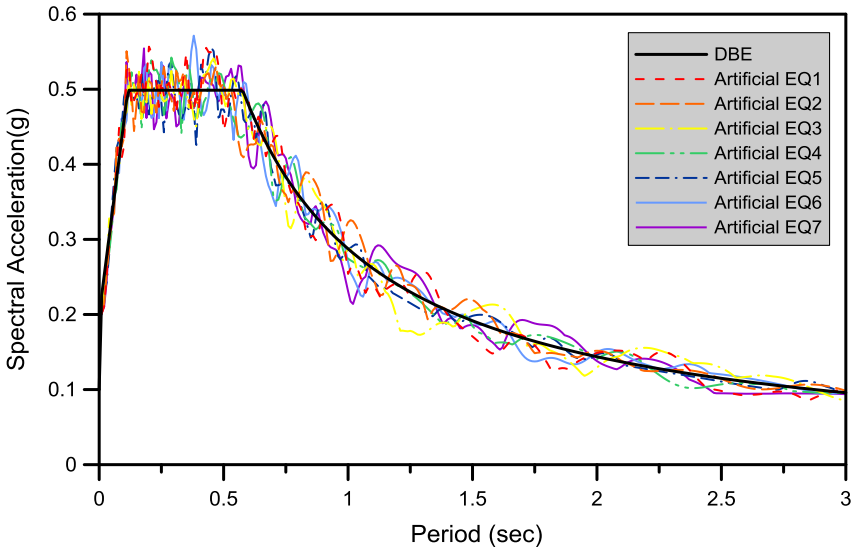

Fig. 12. Response spectra of the artificial earthquake records generated to fit the design spectrum.

on the axial force they resist. Using the effective stiffness, the natural periods of the structure are computed as 2.48 and 2.15 s along the longitudinal and transverse directions, respectively. To evaluate the seismic performance of the structure, the seven artificial earthquake records are generated in such a way that the response spectra of the records match with the design spectrum constructed with the seismic coefficients $S_{DS} = 0.50$ and $S_{D1} = 0.29$. Fig. 12 depicts the response spectra of the artificial earthquake records and the design spectrum. Nonlinear dynamic analyses of the model structures are carried out using the program code Perform 3D [16]. The analysis is performed using step-by-step integration with time step of 0.01 s, using the constant average acceleration method (also known as the trapezoidal rule or the Newmark $\beta = 1/4$ method). The maximum inter-story drifts of the structure obtained from the seven time history analysis results are plotted in Fig. 13. It can be observed that the maximum inter-story drift of the structure along the longitudinal direction is about 1.6 % of the story height, and the drift along the transverse direction is about 2.2 % of the story height. As the responses along the transverse direction far exceed the life safety performance limit state for a hospital building, which is 1.0 % of the story height, it is determined that the structure be retrofitted for earthquake load along the transverse direction (see Fig. 14).

3.2. Evaluation of effective damping required for seismic retrofit

In this section the effective damping ratio required to meet the target performance point for seismic retrofit is estimated using the capacity spectrum or capacity-demand diagram method specified in ASCE/SEI 41-13. The capacity spectrum method (CSM) compares the capacity of a structure to resist lateral forces to the demands of earthquake response spectra in a graphical presentation that

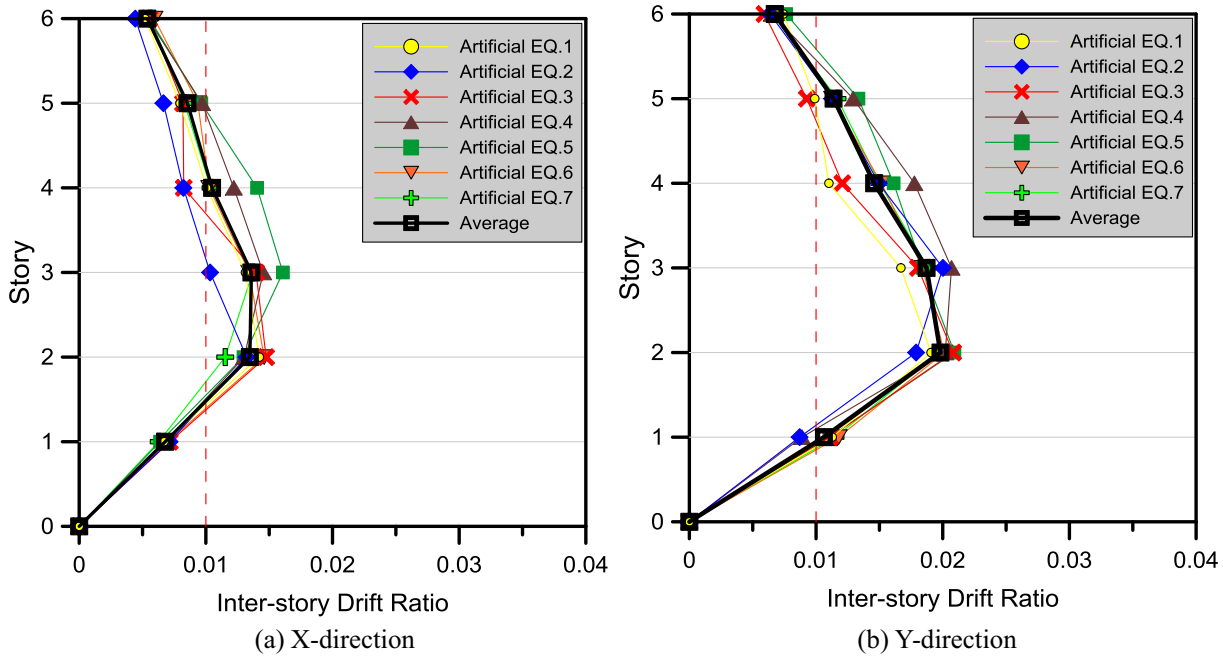

Fig. 13. Inter-story drift ratios of the model structure before seismic retrofit.

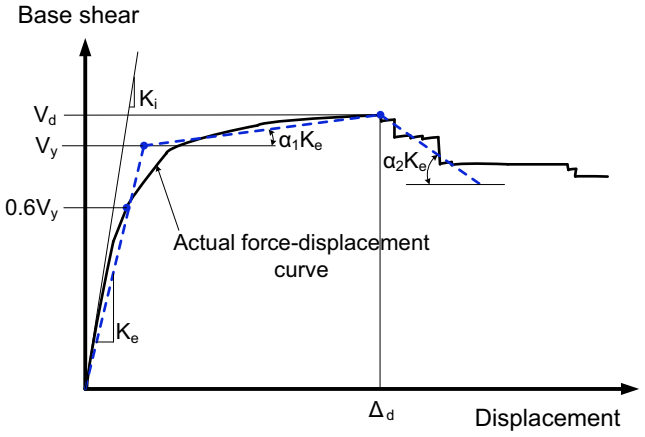

Fig. 14. Idealized force-displacement curve (ASCE/SEI 41-13).

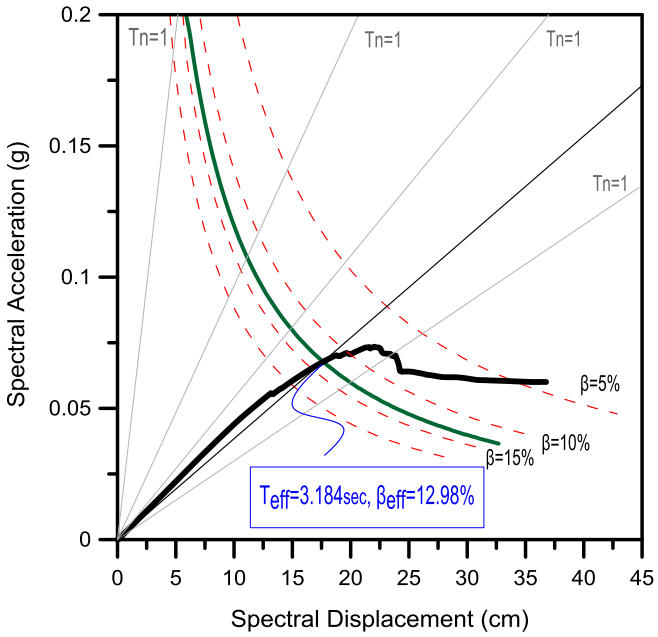

Fig. 15. Performance point of the original structure along the Y-axis obtained from capacity spectrum analysis.

allows a visual evaluation of the seismic performance of the structure. The method is generally used to obtain structural responses without nonlinear dynamic analysis taking into account the nonlinear behavior of structures subjected to strong earthquakes. Pushover analysis is carried out to obtain the nonlinear force-displacement relationship of the structure, which is transformed into a capacity curve, and the demand curve is obtained from the design spectrum. Performance point is determined from the cross point of the two curves. Effective damping ratio is computed at the performance point, which is used to modify the demand curve and to obtain a new performance point. The process is repeated until convergence. The effective period of the structure along the transverse direction is computed to be 2.3 s using the following formula:

$$T_{eff} = T_i\sqrt{\frac{K_i}{K_e}} \tag{2}$$

where T_i is the elastic fundamental period (in seconds) in the direction under consideration calculated by elastic dynamic analysis; K_i is the elastic lateral stiffness of the building in the direction under consideration; and K_e is the effective lateral stiffness of the building in the direction under consideration. Fig. 15 shows the performance point of the original model structure along the transverse direction obtained from capacity spectrum analysis.

In case the target inter-story drift of 1 % of the story height occurs in each story, the roof-story displacement of the structure becomes 225 mm. The corresponding spectral displacement, S_d, is computed to be 101.6 mm using the following formula:

$$S_d = \frac{\Delta_{Roof}}{PF_1 \times \phi_{Roof,1}}, \quad PF_1\frac{\sum_{i=1}^{N} m_i\phi_{i1}}{\sum_{i=1}^{N} m_i\phi_{i1}^2} \tag{3}$$

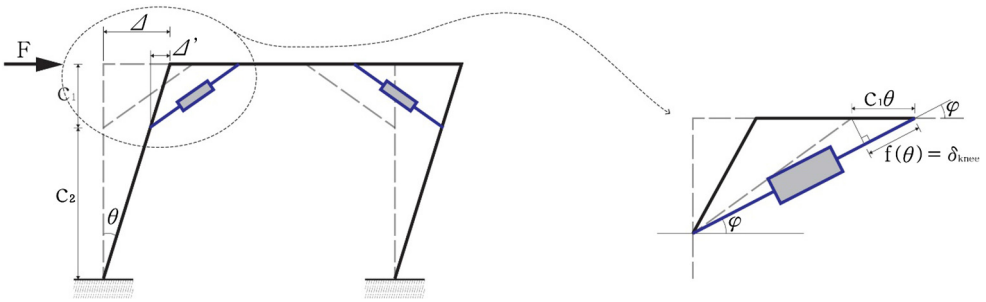

Fig. 16. Axial displacement of the slit damper used as knee braces.

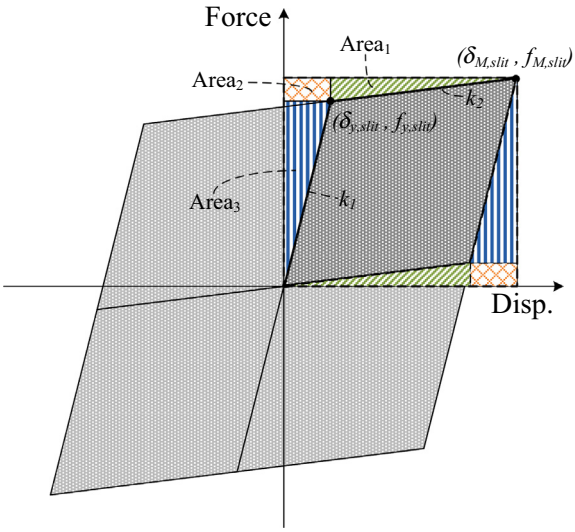

Fig. 17. Graphical derivation of hysteretic energy dissipated by the slit damper per cycle.

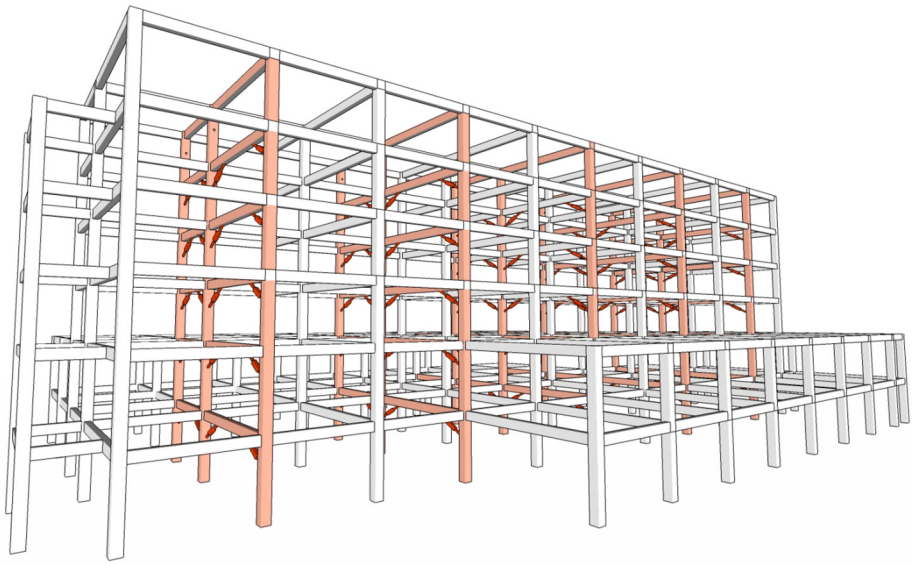

Fig. 18. Locations of the slit dampers in the reinforced analysis model structure.

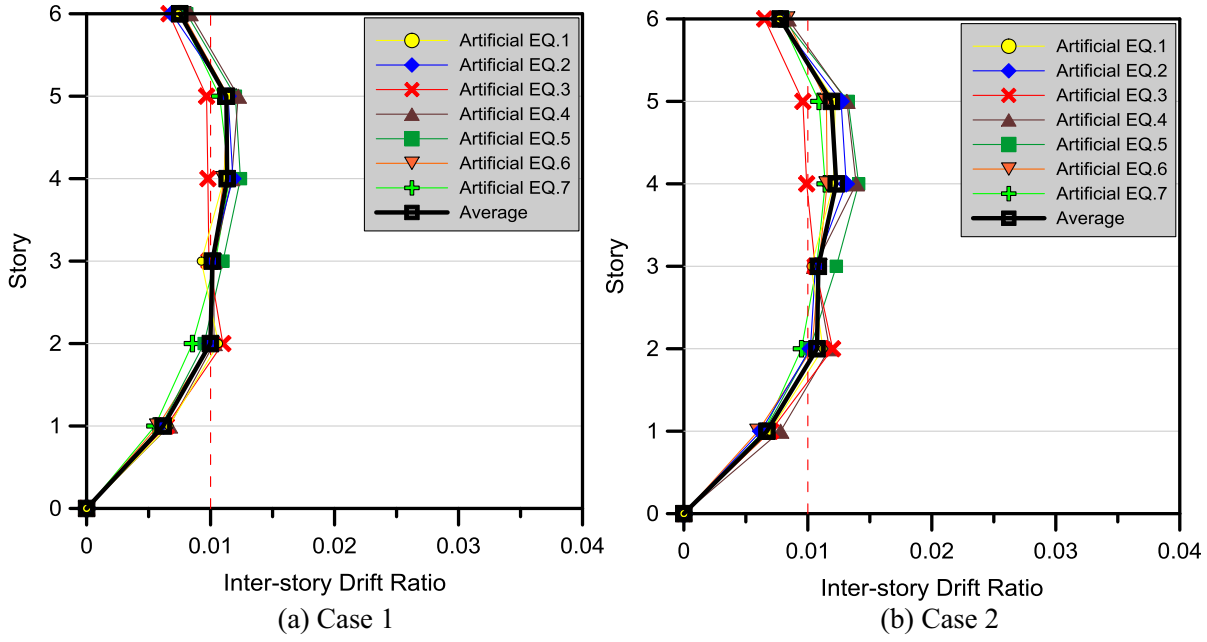

Fig. 19. Inter-story drift ratio of the model structure along the Y direction after retrofitted with the slit dampers.

where Δ_{roof} is the roof displacement, PF_1 is the modal participation factor for the first natural mode, $\phi_{Roof,1}$ and ϕ_{i1} are the roof and ith story components of the first mode shape vector, respectively, N is the number of story, and m_i is the ith modal mass. The effective damping of the structure is obtained as follows [15]:

$$\beta_{eff} = \beta + \frac{\sum E_{Dj}}{4\pi W_k}; \quad W_k = \frac{1}{2}\sum F_i \Delta_i \tag{4a, b}$$

where β = inherent damping, E_{Dj} = work done by the jth damper in one complete cycle of response at the inter-story drift δ_i, W_k = maximum strain energy of the structure when the maximum inter-story drift reaches the target value, F_i = seismic design force at level i, and Δ_i = deflection of level i at the center of rigidity of the structure. Pushover analysis is carried out until the maximum inter-story drift reaches the target value to obtain the story and the inter-story drifts of each story required to estimate the work done by the dampers and the maximum strain energy of the structure.

From the capacity spectrum method, it is observed that the spectral displacement of 101.6 mm is achieved when the effective damping ratio, β_{eff}, is increased to 39% of the critical damping. Assuming that the inherent damping ratio is 5%, the effective damping ratio to be added by the slit dampers to satisfy the performance limit state of 1% of the story height is 34%.

3.3. Design of the slit dampers

The basic principle for designing the dampers is to relate the effective damping ratio required to meet the target performance point, obtained previously, with the energy dissipation made by the dampers with unknown size. Fig. 16 shows the single story

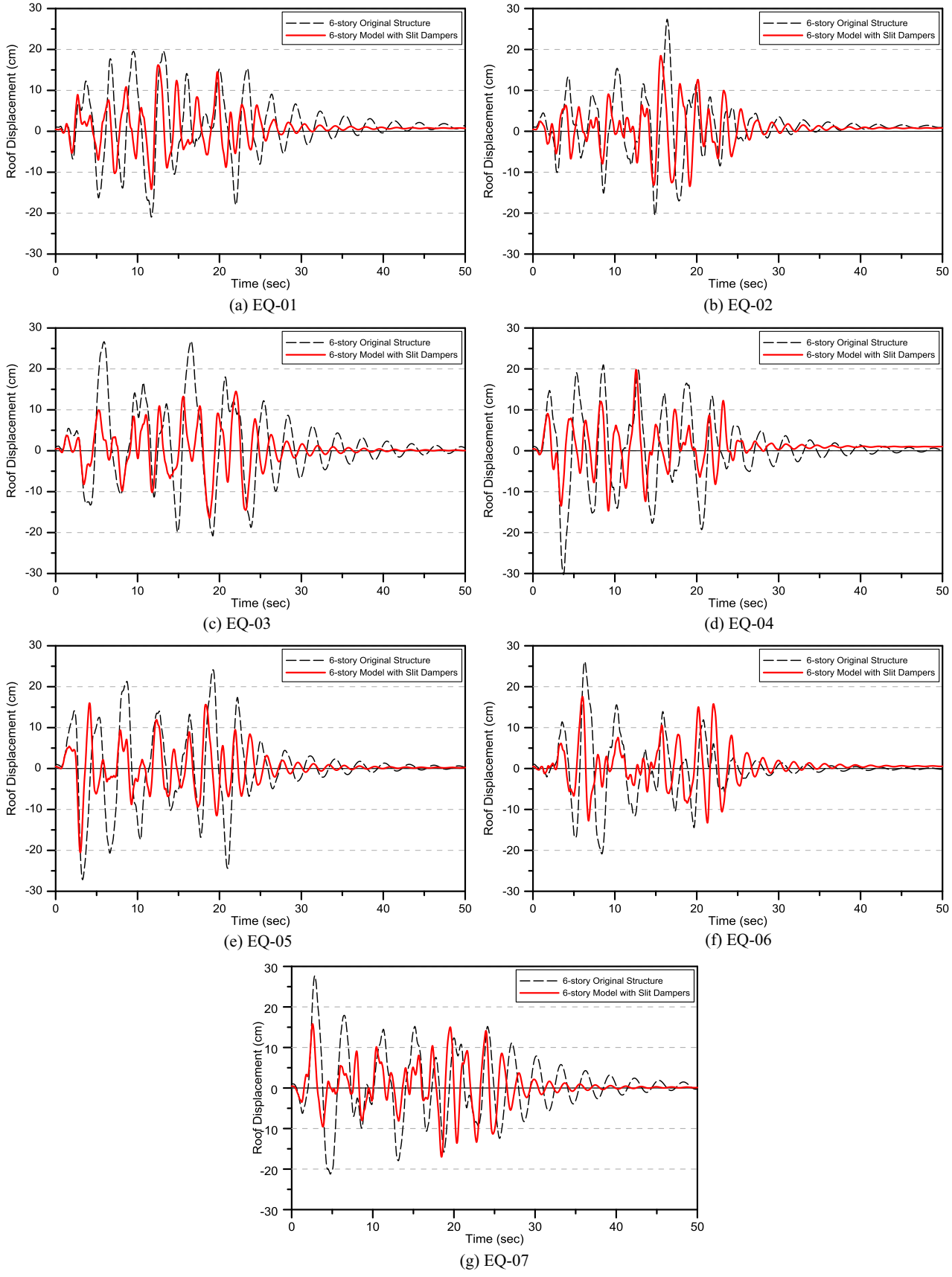

Fig. 20. Roof displacement time histories of the model structure before and after retrofit.

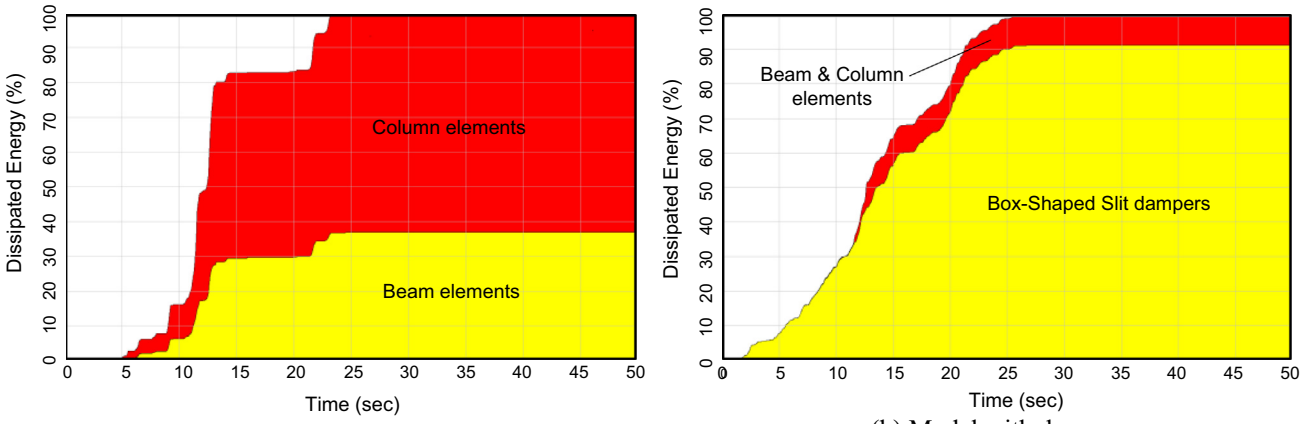

(a) Original model (b) Model with dampers

Fig. 21. Hysteretic energy dissipated by the structural elements when the structure is subjected to the artificial earthquake EQ-1.

structure with slit dampers installed as knee braces at the corners. When the structure is displaced by Δ with lateral drift angle θ, the lateral drift of the knee brace Δ' is $c_1\theta$. In case the knee brace is located at the angle of φ with the beam, the axial displacement of the knee brace, δ_{knee}, is obtained as follows:

$$\delta_{\text{knee}} = c_1\theta \cdot \cos(\varphi) \tag{5}$$

When the knee brace angle is 30° with the beam, the axial displacement of the slit damper corresponding to the inter-story drift ratio of 1% is computed as 8.5 mm. To compute the work done by the dampers, the area of the idealized hysteresis curve in one complete cycle of response shown in Fig. 17 is obtained as follows:

$$\begin{aligned} E_D &= 4 \cdot [(f_{M,slit}\delta_{M,slit}) - (2Area_1) - (2Area_2) - (2Area_3)] \\ &= 4 \cdot [f_{y,slit}\delta_{M,slit} - f_{M,slit}\delta_{y,slit}] \end{aligned} \tag{6a}$$

$$\begin{aligned} &f_{y,slit} = n\frac{\sigma_y t b^2}{2l_0}, \quad \delta_{y,slit} = \frac{\sigma_y l_0^2}{2bE}, \\ &f_{M,slit} = f_{y,slit} + [(\delta_{M,slit} - \delta_{y,slit}) \cdot k_2], \quad \delta_{M,slit} = c_1\theta\cos(\varphi) \end{aligned} \tag{6b}$$

where E_D represents the energy dissipated per one cycle of vibration, which corresponds to the area of the idealized hysteresis curve shown in Fig. 17, and the quantity inside of the bracket in Eq. (6a) corresponds to a quarter of the total area of the hysteresis curve. Eq. (6) can be transformed into the following form:

$$\begin{aligned} E_D &= 4(\alpha+1)[f_{y,slit}(d_{M,slit} - d_{y,slit})] \\ &= 4(\alpha+1)\left[\frac{n\sigma_y t b^2}{2l_0}\right]\left[c_1\theta\cos(\varphi) - \frac{\sigma_y l_0^2}{2bE}\right] \end{aligned} \tag{7}$$

Using the dissipated energy obtained above, the effective damping ratio of the structure with the knee brace slit dampers can be expressed as follows:

$$\beta_{eff} = \beta + \frac{\sum_j 4(\alpha+1)\left[\frac{n\sigma_y t b^2}{2l_0}\right]\left[c_1\theta\cos(\varphi) - \frac{\sigma_y l_0^2}{2bE}\right]}{2\pi\sum_i F_i\delta_i} \tag{8}$$

In case the length of slit column (l_0) is 80 mm, the yield stress of the plate (σ_y) is 0.325 kN/mm^2, the elastic modulus is 2050.0 kN/mm^2, the width of strip (b) is 8 mm, and the dampers are installed at two upper corners as shown in Fig. 16, the thickness of the steel plate (t) required to satisfy the effective damping of 39% is estimated to be 7.8 mm. Based on the result the thickness of the slit plates is determined to be 8 mm in the retrofit design.

4. Seismic performance of the retrofitted structure

To provide the effective damping required to satisfy the target maximum inter-story displacement of 1.0 % of the story height, 100 dampers with yield force of 50 kN per unit are installed along the short direction as shown in Fig. 18. For comparison 50 dampers with yield force of 100 kN per unit are installed only at the interior corners, and the retrofitted structures are analyzed using the seven artificial records generated based on the design spectrum. Fig. 19 shows the maximum inter-story drifts of the model structure retrofitted with 100 of 50 kN dampers (Case 1) and 50 of 100 kN dampers (Case 2). It can be observed that in both cases the maximum inter-story drifts occur at the fourth and the fifth stories, and that the maximum inter-story drifts are slightly larger than the target value of 1.0 % of the story height. However they are significantly reduced compared with the inter-story drifts of the structure before retrofit as can be observed in Fig. 13(b). The mean maximum inter-story drift of Case 1 turns out to be 1.13 % of the story height at the fourth story, which is only 44 % of the mean maximum inter-story drift of the structure before retrofit. Even though the inter-story drifts of the Case 2 structure is slightly larger than those of the Case 1 structure, the difference is almost negligible. Fig. 20 depicts the roof displacement time histories of the model structure before and after retrofit obtained from nonlinear dynamic analysis using the seven earthquake records. It can be observed that the roof displacement is significantly reduced in most earthquake records after the dampers are installed.

Fig. 21 shows the hysteretic energy dissipated by the structural elements and dampers when the structures are subjected to the artificial earthquake record EQ-1. The Case 1 damper installation scheme is considered in the seismic retrofit. It can be noticed that in the original structure 62.8 % of the input seismic energy is dissipated by the inelastic deformation of the columns and the remaining energy is dissipated by the beams. Such strong beam weak column behavior can be frequently observed in the typical building structures not designed for seismic load. It also can be observed that in the structure retrofitted with the 100 knee brace slit dampers, about 90 % of the input energy is dissipated by the dampers and only small amount of energy is dissipated by structural elements. This implies that damage in structural elements is significantly reduced after the dampers are installed, and that the forces transferred to the structural members from the dampers are not large enough to cause yielding of the members. This conforms to the code requirement that the structural elements supporting the dampers remain elastic under design level seismic load.

5. Conclusions

In this study a steel slit damper was developed by combining four steel slit plates into a box shape to be used as a knee brace for seismic retrofit of structures. Cyclic loading tests of the dampers were carried out to evaluate their seismic energy dissipation capability and to develop load-displacement relationship. The slit dampers were applied to seismic retrofit of an existing reinforced concrete structure using the procedure developed based on the capacity spectrum method. The amount of dampers required to meet the limit state for a design basis earthquake was determined from the difference in the equivalent damping ratios corresponding to the performance point and the target point. The seismic performance of the structure before and after the retrofit was evaluated by nonlinear dynamic analysis using seven artificial earthquake records generated to fit the design spectrum.

The test of the two specimens showed that the box type slit dampers had stable energy dissipation capacity with enough deformability as knee braces. Nonlinear dynamic analysis of the model structure showed that the dampers installed using the capacity spectrum-based procedure were effective in restraining the inter-story displacement within a given target performance limit state. The time history of the hysteretic energy showed that most of the input seismic energy was dissipated by the dampers and the structural elements mostly remained elastic. This conforms to the code requirement that the structural elements supporting the dampers remain elastic under design level seismic load. The design process based on the equivalent damping ratios corresponding to the performance point and the target point obtained from the capacity spectrum method turned out to be useful for design of the slit dampers developed in this study.

Acknowledgment

This research was supported by a grant (17CTAP-C132889-01) from Technology Advancement Research Program (TARP) funded by Ministry of Land, Infrastructure, and Transport of Korean government. The tests of the specimens were supported by Teapyung P&E. Those supports are greatly appreciated.

References

[1] Xia C, Hanson RD. Influence of ADAS element parameters on building seismic response. J Struct Eng ASCE 1992;118(7):1903–18.
[2] Park J, Lee J, Kim J. Cyclic test of buckling restrained braces composed of square steel rods and steel tube. Steel Compos Struct 2012;13:423–36.
[3] Choi H, Kim J. Energy-based seismic design of buckling-restrained braced frames using hysteretic energy spectrum. Eng Struct 2006;28(2):304–11.
[4] Lee M, Lee J, Kim J. Seismic retrofit of structures using steel honeycomb dampers. Int J Steel Struct 2017;17(1):215–29.
[5] Kim Y, Ahn T, Kim H, Jang D. Development of new steel damper for seismic retrofit of existing structures. In: 15th world congress of earthquake engineering, Lisboa, Portugal; 2012.
[6] Kobori T, Miura Y, Fukuzawa E, Yamada T, Arita T, Takenaka Y, et al. Development and application of hysteresis steel dampers. In: 10th world conference on earthquake engineering, Rotterdam, Netherland.
[7] Chan RWK, Albermani F. Experimental study of slit damper for passive energy dissipation. Eng Struct 2008;30(4):1058–66.
[8] Saffari H, Hedayatb AA, Poorsadeghi NM. Post-Northridge connections with slit dampers to enhance strength and ductility. J Constr Steel Res 2013;80(1):138–52.
[9] Seo J, Kim Y, Hu J. Pilot study for investigating the cyclic behavior of slit damper systems with recentering shape memory alloy (SMA) bending bars used for seismic restrainers. Appl Sci 2015;5:187–208.
[10] Kim J, Jeong J. Seismic retrofit of asymmetric structures using steel plate slit dampers. J Constr Steel Res 2016;120:232–44.
[11] Lee CH, Lho SH, Kim DH, Oh J, Ju YK. Hourglass-shaped strip damper subjected to monotonic and cyclic loadings. Eng Struct 2016;119(15):122–34.
[12] Lee CH, Ju YK, Min JK, Lho SH, Kim SD. Non-uniform steel strip dampers subjected to cyclic loadings. Eng Struct 2015;99(15):192–204.
[13] Lee J, Kim J. Seismic performance evaluation of moment frames with slit friction hybrid dampers. Earthquakes Struct 2015;9(6):1291–311.
[14] Kim J, Shin H. Seismic loss assessment of a structure retrofitted with slit-friction hybrid dampers. Eng Struct 2017;130(1):336–50.
[15] ASCE/SEI 41-13. American society of civil engineers. Seismic evaluation and retrofit of existing buildings. Reston; 2013.
[16] Perform 3D. Computer and Structures. Inc. PERFORM User Guide ver 4; 2006.